Cooper Minima in the Photoemission Spectra of Solids

S. L. Molodtsov,[1,*] S. V. Halilov,[2] V. D. P. Servedio,[3] W. Schneider,[1] S. Danzenbächer,[1] J. J. Hinarejos,[1,†]
Manuel Richter,[3] and C. Laubschat[1]

[1]*Institut für Oberflächenphysik und Mikrostrukturphysik, TU Dresden, D-01062 Dresden, Germany*
[2]*Electron Physics Group, NIST, Gaithersburg, Maryland 20899-8412*
and School of Physics, Georgia Institute of Technology, Atlanta, Georgia 30332
[3]*Department of Theoretical Solid State Physics, IFW Dresden, P.O. Box 270016, D-01171 Dresden, Germany*
(Received 17 April 2000)

Variations of the photoionization cross section of valence states as a function of interatomic distance are studied by means of atomic and solid-state density functional approaches and compared with photoemission data. In contrast to the free atom case, a series of Cooper minima is found for $4d$, $5d$, and $5f$ states in Pd, Ag, Au, and U metals. The discovered fundamental phenomenon is of high importance for the correct interpretation of photoemission data.

PACS numbers: 78.70.–g, 79.60.Bm

The energy dependence of photoionization cross sections is a tool frequently used to identify contributions from different atomic states to valence-band photoemission (PE) spectra. Particularly useful is the appearance of phenomena such as Fano resonances [1] or Cooper minima (CM) [2] providing a strong enhancement or decrease of the PE signal from certain states. While the Fano resonance is a many-body effect caused by coupling of the direct PE channel with photoexcitations into localized intermediate states and subsequent autoionization, the CM represents a simple matrix element effect: Due to a node of the initial-state wave functions the transition matrix element into final states with oscillating free-electron-like wave functions becomes canceled. The behavior of the cross section around the CM depends strongly on the shape of the initial-state waves. Atomic calculations by Yeh and Lindau [3] (denoted YL in the following) provide the photoionization cross sections for all elements of the periodic table in a wide range of photon energies. Thereby, not more than one CM is found for any atomic shell considered.

In solids, however, valence states reveal much less pronounced Cooper minima than the related states in the free atoms [4–9]. Additionally, CM in solids are shifted in energy and broadened as compared to their positions and widths in free atoms. These solid-state phenomena have been discussed primarily in terms of hybridization effects [4–7,9]. Another very important difference between free atoms and solids has been, however, completely ignored in the discussion so far: the different symmetry of atomic and solid-state wave functions. For free atom bound states, the amplitudes of the electron wave functions decay exponentially at large distance to the nucleus, and transition matrix elements are calculated by integration over the whole space. In a solid, periodic Bloch states are formed and for direct transitions all translationally equivalent Wigner-Seitz (WS) cells give the same contributions to the integral. This difference should heavily affect the conditions for the appearance of CM.

In the present Letter we show that the translational symmetry may cause a series of Cooper minima in solids instead of a single one known to exist in the free atom. We find experimentally the existence of more than one CM for $4d$ states of Pd and Ag metals and reproduce the phenomenon by atomic and solid-state density functional calculations. Similar effects are predicted for the $5d$ bands of Au metal. Particular attention is paid to the $5f$ states of U metal, where CM effects are found to superimpose the $5d \rightarrow 5f$ Fano resonance. We show that proper consideration of solid-state phenomena in PE cross sections is not only crucial for a correct identification of different valence-band contributions but is also important for the understanding of many-body phenomena in PE spectra.

The experiments were performed at the PM5 beam line of the Berliner Elektronenspeicherring für Synchrotronstrahlung (BESSY I). In order to avoid band structure or possible photoelectron diffraction effects, polycrystalline samples, which were prepared by *in situ* thermal deposition of about 500 Å Pd or Ag onto a Cu substrate at a pressure better than 2×10^{-8} Pa, were studied. Since polycrystalline solids do not have any preferential direction, the angular distribution of the Pd and Ag $4d$ PE is expected to be governed by Yang's theorem [10]. The influence of the asymmetry parameter was eliminated by recording spectra close to the so-called "magic" angle of 54.7° between the axis of electron detection and polarization vector of the incoming photon beam. The spectra were taken in an angle-integrated mode using a hemispherical electron-energy analyzer with an acceptance angle of ±14°. The light was at near-normal incidence to the sample, so that reflectivity corrections were negligible. The valence-band PE spectra of Pd and Ag metals were normalized to the total PE signal of the $3d$ bands of polycrystalline Cu metal measured in the same experimental setup [11]. For the Cu $3d$ states themselves no distorting CM-like cross-section variations in the photon-energy range of interest are expected from our model calculations.

We consider first the case of the $4d$ states of Pd, which show clearly bandlike behavior in solids. The numerical investigations are kept as simple as possible in order to focus the attention to the most essential point: the difference between atomic and solid situations. We adopt a single electron approximation in the calculation of the dipole matrix elements,

$$M_{4d\to\varepsilon f,\varepsilon p} \sim (\varepsilon - \varepsilon_{4d}) \int \psi^*_{4d}\mathbf{r}\psi_{\varepsilon f,\varepsilon p}\, d^3r\,, \quad (1)$$

as was done in the original work by Cooper [2]. Here, ψ_{4d} is the single-particle wave function of the initial $4d$ state and $\psi_{\varepsilon f,\varepsilon p}$ is the wave function of the outgoing electron with f or p character. The related energies are ε_{4d} and ε, respectively. The additional energy dependence of $M_{4d\to\varepsilon f,\varepsilon p}$ from the partial joint density of states is not considered in Eq. (1). Unlike [2,3], where Hartree-Fock wave functions were used, we employ the local density approximation (LDA) known to work well in the case of weakly correlated systems. For free atoms, the mentioned difference leads to a minor shift of the CM of the Pd $4d$ states from 115 [3] to 114 eV. A much more important difference from the previous works is that we now identify both the initial and the outgoing wave functions with Bloch states. This reduces the integral in Eq. (1) to an integral over the WS cell, times the number of cells, if only direct transitions are considered; further, in the atomic sphere approximation (ASA), the radial part of the dipole matrix elements is

$$M^r_{4d\to\varepsilon f,\varepsilon p} = (\varepsilon - \varepsilon_{4d}) \int_0^{r_0=r_{ws}} R_{4d} r R_{\varepsilon f,\varepsilon p} r^2\, dr\,. \quad (2)$$

Radial wave functions are obtained by outward integration of the Dirac equation at fixed energies $\varepsilon_{4d} = E_F$ (Fermi energy) and ε, respectively, and matching to spherical functions at the WS cell radius, r_{ws}. The scalar relativistic functions R_{4d} and $R_{\varepsilon f,\varepsilon p}$ are defined in such a way that R^2 is equal to the average of $j = l \pm 1/2$ radial densities. The result is not sensitive to variations of ε_{4d} within the $4d$ bandwidth. The potential entering the Dirac operator is obtained from a relativistic linearized muffin-tin orbital (LMTO)-ASA-LDA calculation. In the following we refer to the described procedure as solid-state calculation. Alternatively, the potential is obtained from a relativistic free atom self-interaction corrected-LDA calculation, R_{4d} is a bound state atomic radial wave function, and $R_{\varepsilon f,\varepsilon p}$ is the f or p component of an outgoing spherical wave. This approach we refer to as our atomic calculation.

PE intensity variations of the Pd metal valence-band signal measured close to E_F [0.3 eV binding energy (BE)] and at 1.4 eV BE as a function of photon energy ($h\nu = \varepsilon - \varepsilon_{4d}$) are shown in the middle of Fig. 1 (open and solid circles, respectively). The two presented experimental dependences reveal qualitatively similar behavior showing that the joint density of states has only a minor influence

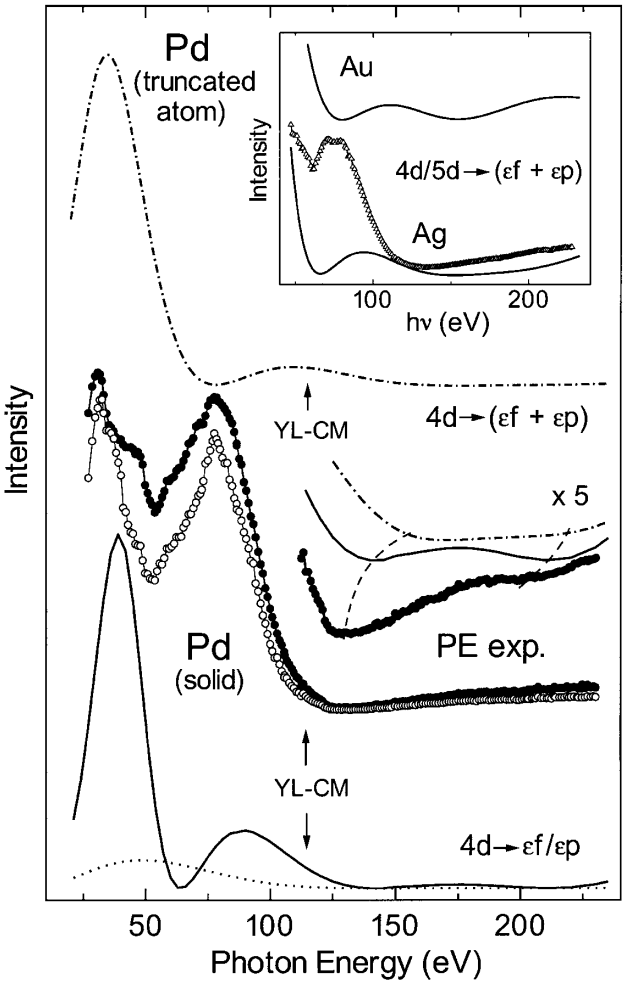

FIG. 1. Pd valence-band PE intensities measured at 0.3 eV (open circles) and 1.4 eV (solid circles) BE for different $h\nu$. Results of solid-state calculations of $|M^r_{4d\to\varepsilon f}|^2$ (solid line) and $|M^r_{4d\to\varepsilon p}|^2$ (dotted line) for $r_{ws} = 1.52$ Å are shown in the bottom. Results of our atomic approach for the $4d \to (\varepsilon f + \varepsilon p)$ transitions calculated with an integration limit $r_0 = 1.52$ Å are plotted at the top (dash-dotted line). The energy position of the YL-CM is marked by vertical arrows. In the middle, our theoretical solid-state ($r_{ws} = 1.52$ Å) and atomic ($r_0 = 1.52$ Å) results in the region of high $h\nu$ (solid and dash-dotted lines, respectively) are compared, with a magnification 5, to the experimental data taken at 1.4 eV below E_F. The inset shows by solid lines the results of our atomic calculations for Au ($r_0 = 1.55$ Å) and Ag ($r_0 = 1.55$ Å) metals. Open triangles denote Ag $4d$ integral PE intensity variations measured in the present study.

on the cross-section variations in the photon-energy range considered. In order to emphasize weak details in the region of high $h\nu$, the corresponding part of the 1.4-eV curve is also plotted with a magnification 5. As seen in the figure, the calculated atomic YL-CM at 115 eV has a counterpart in the experimental solid-state data. It is shifted, however, toward higher $h\nu$ as was already observed in previous studies of Pd [6] and other transition [4,5] and noble metals [6]. Besides this feature, which is the only minimum obtained from the atomic YL calculations [3], another pronounced minimum is observed around 50 eV photon energy in the

experimental data. In previous publications dealing with the Cooper-minimum phenomenon in transition and noble metals this energy range was usually not studied or only a small number of experimental points were taken [4–7] that did not allow one to monitor the structure observed in the present experiment. To our knowledge, there are only a few studies where the low photon energy region was carefully investigated and a related feature was also detected [11,12]. In these publications, the low-energy structure was simply assigned to general "solid-state effects" without deeper investigation of their origin.

The solid-state calculations performed in the present study show unambiguously that similar to the classic CM this experimentally observed structure is caused by the radial part of the dipole matrix elements, Eq. (2). The results of our matrix-element calculations for fcc Pd metal ($r_{ws} = 1.52$ Å) are shown in the bottom of Fig. 1. In contrast to the YL data, the corresponding theoretical solid-state curve for the $4d \rightarrow \varepsilon f$ transition (solid line) reveals several minima at 65, 142, and 218 eV. The $4d \rightarrow \varepsilon p$ transitions (dotted line) are about 1 order of magnitude less intense than the $4d \rightarrow \varepsilon f$ transitions. The middle minimum of the solid curve in the bottom is located close to the energy of the conventional CM [3], whereas another one lies in the region of the low-energy structure observed in the present experiment. Careful inspection of the experimental data in the region of high $h\nu$ reveals an additional although rather weak feature, which is found near the third minimum calculated at 218 eV with the solid-state approach (see curves shown with magnification).

As a result all minima predicted by the solid-state calculations are found in the experiment. Deviations of the intensity between theory and experiment as well as fine structures in the region of the 50-eV minimum seen only in the experimental curves can be explained by contributions of states with other than $4d$ and εf angular-momentum characters to the experimental PE intensity and by the fact that the theoretical curve represents only the radial part of the dipole matrix element. We emphasize, therefore, that our present model calculations provide trustworthy data for only the number and energy positions of the solid-state CM. Extended calculations of $M_{4d\rightarrow\varepsilon f}$ will be presented in a forthcoming publication. Here, we give only a transparent guide through the observed phenomena along a series of metals with $4d$, $5d$, and $5f$ valence states. To this end we follow the transition of the observed series of solid-state CM into the single CM in the gas phase by increasing the interatomic distances between neighboring Pd atoms. A comparison between theoretical solid-state results for $r_{ws} = 1.52$ Å and a model value $r_0 = 1.95$ Å (not presented) shows that the calculated Pd $4d$ minima are shifted toward lower $h\nu$ in the expanded solid. Thereby the middle minimum approaches the position of the classic Cooper minimum of the free atom (YL-CM). We underline, however, that by several solid-state calculations ($1.52 < r_0 < 1.95$ Å) we obtained a series of CM. Since further expansion of the solid is treacherous within the LMTO-ASA-LDA approach, the matrix elements for larger interatomic distances were estimated using atomic calculations setting the integration limit, r_0, at increasing distances from the core [13]. Results of our atomic calculations for $r_0 = 1.52$ Å are shown at the top in Fig. 1. As is evident from the figure, our atomic and solid-state approaches are virtually equivalent. The atomic calculations reveal three minima as well, which are slightly shifted, however, toward higher $h\nu$ as compared to their positions derived from the solid-state calculation.

The evolution of the CM with r_0 as obtained from our atomic approach is shown in Fig. 2. The observed behavior is evidently characterized by some kind of periodicity. At small distances, a series of discrete CM is obtained that move to lower energies with increasing r_0 and disappear abruptly below a certain energy $h\nu$. In the region between 120 and 160 eV photon energies, the individual CM split into two components, from which the stronger one joins the previous lower lying CM, while the weaker component merges in the next higher lying one. At large distances, the CM at high $h\nu$ become less and less pronounced, and only in the region of merging a broad minimum remains, which corresponds to the classic CM obtained for the free atom [3]. The reason for the observed periodic behavior is

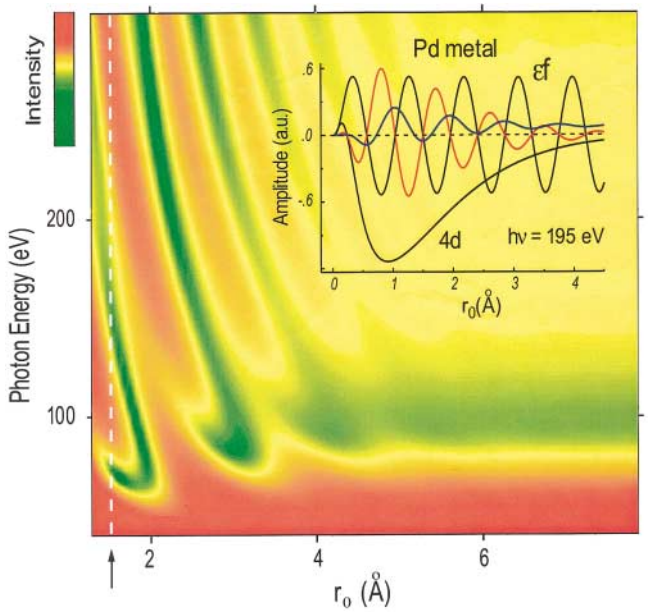

FIG. 2 (color). $|M^r_{4d\rightarrow(\varepsilon f+\varepsilon p)}|^2$ of Pd calculated with our atomic approach for different $h\nu$ and distances r_0. The CM are represented by green color (see intensity scale). The white broken line and vertical arrow mark a cut at $r_0 = 1.52$ Å corresponding to the curve presented at the top of Fig. 1. Results of our atomic approach for $r_0 > 5$ Å are almost equivalent to those of the atomic YL calculations. The inset shows the radial parts of wave functions for the final (εf, multiplied with r) and initial ($4d$, multiplied with r^2) states as well as the integrand (red curve) and the integral (blue curve) of Eq. (2).

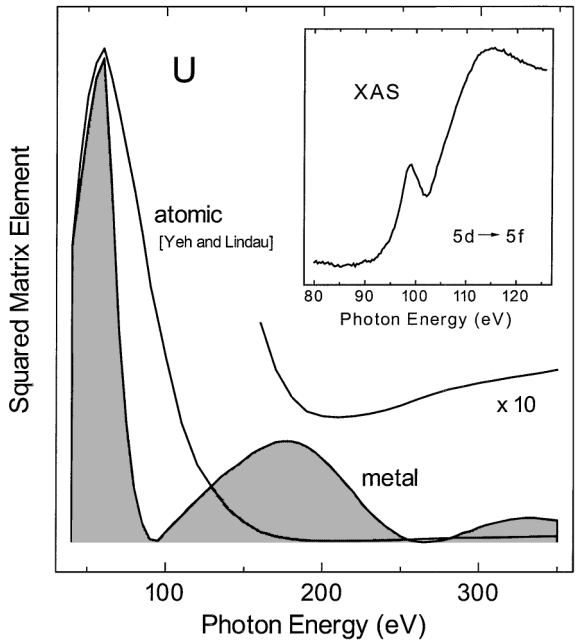

FIG. 3. $|M^r_{5f\to\varepsilon g}|^2$ ($M^r_{5f\to\varepsilon d}$ is negligible) for hcp U metal ($r_{ws} = 1.70$ Å) calculated with the solid-state approach (shadowed area) in comparison to the YL results (solid line). The latter are presented also in the region of the CM with a magnification 10. The inset shows an x-ray absorption spectrum taken in electron yield mode in the region of the U $5d \rightarrow 5f$ excitation threshold.

visualized in the inset in Fig. 2. For a given photon energy ($h\nu = 195$ eV), both initial- and final-state radial wave functions (black curves) as well as the integrand of Eq. (2) (red curve) are plotted as a function of r_0. The integrand reveals the same oscillatory character as the final state with the amplitude following the intensity of the initial-state wave function. A corresponding damped oscillatory behavior of the matrix element (blue curve) causing the appearance of a series of CM is obtained upon integration of Eq. (2).

The presented combination of the solid-state and atomic calculations allows one to understand the mechanism of the CM in solids. It shows also that our atomic approach can be successfully used for a simple express analysis of the CM behavior in solids. Corresponding results of our atomic calculations of squared dipole matrix elements for another $4d$ metal, Ag, and a $5d$ metal, Au, are shown in the inset in Fig. 1. Two CM observed theoretically both for Ag and Au metals at 60–80 eV and 150–160 eV are in good agreement with previously published experimental results [11,12], as well as with our own experimental data taken for the $4d$ states of Ag.

The appearance of more than one CM can also be expected for $5f$ states of solid U systems that reveal to a certain degree bandlike properties [14]. Results of solid-state calculations for the $5f$ states of hcp U metal are shown in Fig. 3. In contrast to the free atom YL calculation that yields only one CM at 210 eV, our solid-state approach gives for $h\nu < 350$ eV two CM at about 90 and 265 eV photon energies. It is important to note that the low lying CM appears in a photon energy range immediately below the U $5d \rightarrow 5f$ threshold (see inset in Fig. 3). This fact has severe consequences for the quantitative interpretation of resonant PE data taken at this threshold in U systems: Until now, an experimentally observed drastic decrease of the U $5f$ PE intensity in the region of $h\nu = 90$–94 eV has exclusively been attributed to the $5d \rightarrow 5f$ Fano antiresonance [15]. From the depth and position of the antiresonance the Fano asymmetry parameter can be derived, which in turn allows one to draw conclusions about the localization of the $5f$ wave functions. With the new mechanism in mind these conclusions will possibly have to be revised.

This work was supported by the Deutsche Forschungsgemeinschaft, Sonderforschungsbereich 463, TP's B4 and B11, and Graduiertenkolleg "Struktur- und Korrelationseffekte." Valuable discussions with Yu. Kucherenko are gratefully acknowledged.

*On leave from Institute of Physics, St. Petersburg State University, 198904 St. Petersburg, Russia.
†On leave from Departamento de Fisica de la Materia Condensada, Universidad Autonoma de Madrid, E-28049 Madrid, Spain.

[1] U. Fano, Phys. Rev. **129**, 1866 (1961).
[2] J. W. Cooper, Phys. Rev. **128**, 681 (1962).
[3] J. J. Yeh and I. Lindau, At. Data Nucl. Data Tables **32**, 1 (1985).
[4] I. Abbati *et al.,* Phys. Rev. B **32**, 5459 (1985).
[5] I. Abbati *et al.,* Phys. Rev. Lett. **50**, 1799 (1983).
[6] G. Rossi *et al.,* Phys. Rev. B **28**, 3031 (1983).
[7] M. Ardehali and I. Lindau, J. Electron Spectrosc. Relat. Phenom. **46**, 215 (1988); M. Ardehali *et al.,* Phys. Rev. B **39**, 8107 (1989).
[8] T. A. Carlson *et al.,* J. Chem. Phys. **79**, 2157 (1983).
[9] R. J. Cole *et al.,* Phys. Rev. B **46**, 3747 (1992).
[10] C. N. Yang, Phys. Rev. **74**, 764 (1948).
[11] Tschang-Uh Nahm *et al.,* Phys. Rev. B **51**, 8140 (1995); Tschang-Uh Nahm *et al.,* Phys. Rev. B **52**, 16 466 (1995); Tschang-Uh Nahm *et al.,* Phys. Rev. B **54**, 7807 (1996).
[12] W. Folkerts *et al.,* J. Phys. F **17**, 657 (1987).
[13] Yu. N. Kucherenko, J. Electron Spectrosc. Relat. Phenom. **72**, 181 (1995).
[14] S. L. Molodtsov *et al.,* Phys. Rev. B **57**, 13 241 (1998).
[15] B. Reihl *et al.,* Phys. Rev. B **26**, 1842 (1982); A. J. Arko *et al.,* Phys. Rev. B **27**, 3955 (1983); J. W. Allen *et al.,* Phys. Rev. Lett. **54**, 2635 (1985).